



## Phytoplankton and light limitation in the Southern Ocean: Learning from high-nutrient, high-chlorophyll areas

Hugh Venables<sup>1</sup> and C. Mark Moore<sup>2</sup>

Received 6 March 2009; revised 18 September 2009; accepted 2 October 2009; published 27 February 2010.

[1] Most of the Southern Ocean is a high-nutrient, low-chlorophyll (HNLC) area. There are exceptions to this situation downstream of some of the islands, where iron from the islands or surrounding shallow plateau fertilizes the mixed layer and causes a phytoplankton bloom in spring and summer. The main locations where this occurs are downstream of the South Georgia, Crozet, and Kerguelen islands. Data on mixed layer depths from Argo float profiles together with Sea-viewing Wide Field-of-view Sensor chlorophyll *a* (chl *a*) and photosynthetically available radiation from these high-nutrient, high-chlorophyll (HNHC) areas are combined to study the effects of mixed layer-averaged light availability on phytoplankton concentrations in areas where iron limitation has been lifted. The results of this analysis are then transferred to HNLC areas to assess the potential importance of light limitation through the year. We conclude that light limitation does not significantly constrain the annual integrated standing stock of chl *a* in the HNLC Southern Ocean.

**Citation:** Venables, H., and C. M. Moore (2010), Phytoplankton and light limitation in the Southern Ocean: Learning from high-nutrient, high-chlorophyll areas, *J. Geophys. Res.*, 115, C02015, doi:10.1029/2009JC005361.

### 1. Introduction

[2] The Southern Ocean has high-macronutrient concentrations because of a large upwelling of nutrient-rich deep water [Pollard *et al.*, 2006]. These are not fully utilized by phytoplankton because of iron limitation [de Baar *et al.*, 2005; Martin, 1990; Martin *et al.*, 1990], brought about by low dust inputs combined with the low solubility of iron leading to iron:nitrate ratios in the upwelled water being below those required by phytoplankton [Duce and Tindale, 1991; Jickells *et al.*, 2005]. The widespread iron limitation leads to generally low chlorophyll *a* (chl *a*) concentrations [Moore *et al.*, 1999], so the area (Figure 1), along with the subarctic and equatorial Pacific, is termed high nutrient, low chlorophyll (HNLC).

[3] The open ocean fertilization experiments so far performed in HNLC regions have unequivocally established that phytoplankton biomass and productivity increase following the addition of iron to these systems [Boyd *et al.*, 2000, 2004; Coale *et al.*, 1996, 2004; Gervais and Riebesell, 2002; Tsuda *et al.*, 2003]. Studies of naturally occurring blooms in HNLC regions have also all reached similar conclusions as to the importance of iron [Blain *et al.*, 2007; Houghton *et al.*, 2005; Korb and Whitehouse, 2004; Planquette *et al.*, 2007]. However, despite the unequivocal evidence for the importance of iron, there remains debate or uncertainty within the literature on the extent to which iron limitation

and/or light limitation are responsible for the maintenance of the HNLC condition in the Southern Ocean. [Aumont and Bopp, 2006; Boyd *et al.*, 2007; de Baar *et al.*, 2005; Mitchell *et al.*, 1991; Platt *et al.*, 2003]. This is, in part, caused by deep mixed layers that occur in the region and the lack of year-round mixed layer data from the area, before the Argo era.

[4] Although iron has been shown to be the proximal limiting factor for Southern Ocean productivity, iron, light, and grazing are all potentially interrelated. The ecumenical iron hypothesis [Morel *et al.*, 1991] proposes that low-iron concentrations force a shift toward smaller phytoplankton species, with higher surface area:volume ratios and hence higher iron uptake:iron demand ratios [Fennel *et al.*, 2003]. These small phytoplankton are more easily grazed, and the rapid growth rate of microzooplankton potentially allows grazing control to be dominant. Because of the requirements for iron in the photosynthesis electron transfer system [Strzepek and Harrison, 2004], iron demand will also be a function of light availability [Maldonado *et al.*, 1999; Raven, 1990; Sunda and Huntsman, 1997]. Cellular iron demand thus increases at low light levels because of the increased chl:carbon ratio needed to capture sufficient photons. Under iron limitation, full acclimation to low light may therefore not be possible, leading to an effective colimitation [Sunda and Huntsman, 1997].

[5] The theoretical basis of light limitation within a nutrient-replete oceanic mixed layer is well established [Huisman *et al.*, 1999; Mitchell *et al.*, 1991; Sverdrup, 1953]. However, the practical application of these theoretical treatments to the natural dynamic mixed community situation is highly problematic [Smetacek and Passow, 1990]. Irrespectively, as phytoplankton biomass and pig-

<sup>1</sup>British Antarctic Survey, Cambridge, UK.

<sup>2</sup>National Oceanography Centre, University of Southampton, Southampton, UK.

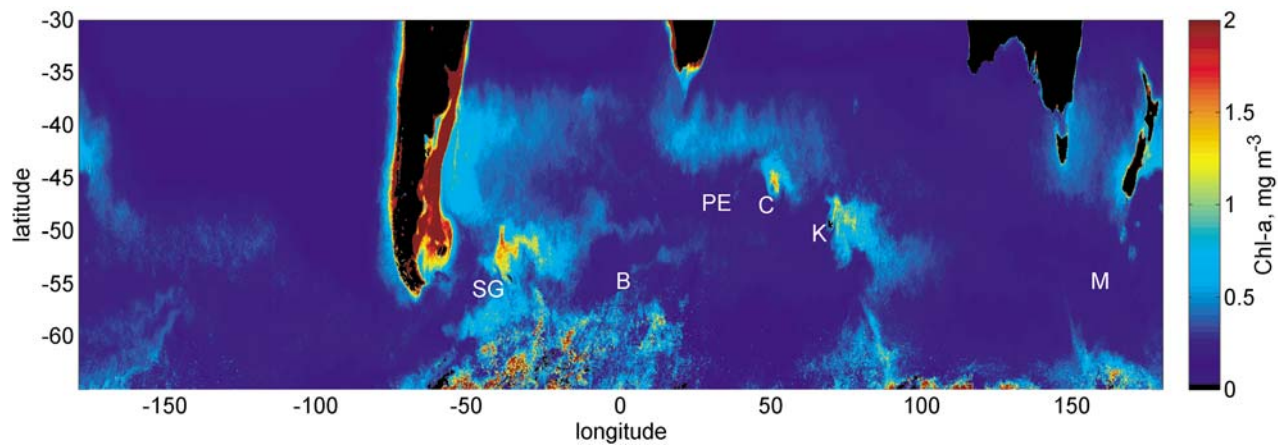


**Figure 1.** Composite SeaWiFS chl *a* image from October to December, 1997–2007. The subantarctic island systems of South Georgia (SG), Bouvet (B), Prince Edward (PE), Crozet (C), Kerguelen (K), and Macquarie (M) are indicated.

ment increase within a mixed layer, the attenuation of light also increases, shoaling the depth over which there is sufficient irradiance for net growth to occur. Hence, within a nutrient-replete mixed layer, simple models, which typically assume loss terms as a constant proportion of phytoplankton standing stock terms, predict that phytoplankton self-shading can lead to a steady state chl *a* concentration, which is inversely related to the mixed layer depth. This has been shown in microcosm experiments [Huisman, 1999]. This inverse relationship is in potential agreement with observed relationships in the iron addition experiments [Aumont and Bopp, 2006; de Baar et al., 2005].

[6] Light availability in the mixed layer is described in a number of ways in the literature. This is well summarized by Lalli and Parsons [1997]. The mixed layer depth can be compared to the euphotic (typically where subsurface light is 1% or 0.1% of surface light), compensation (depth of light level where photosynthesis balances loss terms), or critical (depth of mixed layer that would lead to vertically averaged photosynthesis balancing loss terms) depth. Of these, only the last one gives information about the potential for net population growth, and even then, careful consideration of the sum of all loss terms, including grazing, aggregation, and sinking, is required [Smetacek and Passow, 1990]. Moreover, the critical depth will be a function of the surface photosynthetically available radiation (PAR), so any attempt to establish it empirically, and subsequently apply this to other areas, requires that variations in surface PAR be accounted for. Equally, irradiance levels could be considered at the surface or base of the mixed layer or averaged vertically through the mixed layer [Sverdrup, 1953]. The last of these measures, the mean mixed layer irradiance ( $\bar{I}_{MLD}$ ), includes information from surface irradiance and the mixed layer depth and is a good approximation to the light levels experienced by phytoplankton cells as they mix vertically through the mixed layer. By comparing increases in  $\bar{I}_{MLD}$  and chlorophyll, at times of the year when it is expected that light levels are close to limiting, it is possible to find a critical value, which is frequently referred to as the community compensation irradiance ( $I_C$ ).

[7] Within a mixed water column, net growth, leading to pigment and biomass accumulation, will occur provided that the integrated photosynthetic rate is greater than the integrated community, including heterotrophic, respiration, and other loss terms [Siegel et al., 2002; Smetacek and Passow, 1990; Sverdrup, 1953]. As photosynthesis is typically assumed to have a stronger light dependence than the loss terms (in classical Sverdrup theory, loss terms are considered a constant proportion of biomass), these processes will balance at some light level, the compensation irradiance ( $I_C$ ). Net growth is then expected to occur when the vertically averaged mixed layer irradiance ( $\bar{I}_{MLD}$ ) is greater than  $I_C$  [Sverdrup, 1953; Siegel et al., 2002]. That is, a net increase in phytoplankton biomass and hence, to first approximation, chlorophyll would be expected when the average light available to the phytoplankton being mixed up and down in the mixed layer is sufficient for the gross growth to exceed loss. Such an argument is directly comparable to the critical depth criterion but has the advantage that it is applicable under differing surface PAR and mixed layer depths.

[8] Using time series of chl *a* and light,  $I_C$  can be estimated [Siegel et al., 2002], although such estimates may be biased low as blooms can start at the onset of a quiescent surface layer that precedes stratification [Huisman et al., 1999]. Such empirical approaches remove the problem of theoretically calculating  $I_C$  from estimates of the balance between growth and loss terms, which will include poorly constrained processes such as photorespiration and grazing rates. However, it should be recognized that the derived value of  $I_C$  will reflect a composite property of the entire planktonic community, which could, consequently, be influenced by a range of both autotrophic and heterotrophic ecophysiological processes [Smetacek and Passow, 1990].

[9] In this paper, we assess the potential for light availability to be a limiting factor on the annual net accumulation of biomass in the ice-free Southern Ocean. We calculate  $\bar{I}_{MLD}$  from Argo mixed layer depths, Sea-viewing Wide Field-of-view Sensor (SeaWiFS) PAR, and chl *a* from SeaWiFS and Moderate Resolution Imaging Spectroradiometer (MODIS).

We then compare light levels between high- and low-chlorophyll areas. This relies on the reasonable assumption that bloom areas must represent areas and times where sufficient light was available for net phytoplankton accumulation and that the circumpolar nature of the Southern Ocean controls for many physical, chemical, and grazing effects on the mixed layer environment for phytoplankton between high- and low-chlorophyll areas. From this analysis, we assess the potential for seasonal light limitation across the entire Southern Ocean.

## 2. Data

[10] All Argo profiles prior to 1 November 2008 for the area south of 40°S ( $n = 66588$ ) were obtained from [http://www.usgodae.org/cgi-bin/argo\\_select.pl](http://www.usgodae.org/cgi-bin/argo_select.pl) or <http://www.coriolis.eu.org/cdc/default.htm>. As Argo floats need to surface to transmit data, profiles are only available in ice-free areas. Moreover, sea ice damages generically designed Argo floats, so few data are available close to the ice edge as floats are not set there and are likely to break if they drift into such a region. No subice data from specially designed ice-capable floats have been included, but there are some ice edge profiles in the main Argo data set from these floats. Floats drift for 10 days at 1000 or 2000 m between profiles, so data are also restricted to depths deeper than 1000 m, except for a small number of floats that beach on shelves but continue profiling. The scope of this work is therefore the ice-free Southern Ocean deeper than 1000 m. As real-time data that have not been thoroughly checked have been included, further checking was done beyond the quality flags during the processing to exclude profiles where the mixed layer cannot be found, leaving 59,673 profiles.

[11] These profiles are used to find the mixed layer depth, defined as a change of density ( $\Delta\sigma$ ) of  $0.05 \text{ kg m}^{-3}$  relative to the surface. Defining the mixed layer depth is inevitably arbitrary, to some extent, as there is no consistent shape to stratification in the surface layers of the ocean [Brainerd and Gregg, 1995]. Kara *et al.* [2000] found varying criteria for different areas. The density difference used in this study is similar to that used by Kara *et al.* [2003] for surface temperatures typical of the Southern Ocean and matches the lowest difference used by Brainerd and Gregg [1995]. A constant density criterion is preferred as it is density stratification that will determine the vertical mixing dynamics of water parcels, and hence phytoplankton, in the surface layer of the ocean. Investigation of Argo profiles around the Crozet Islands [Venables *et al.*, 2007] found the criterion we use to be the most suitable in that area. The coarse vertical resolution of Argo profiles precludes use of gradient-based criteria. As the light criteria used in this study are found and applied using the same data set, the overall conclusions are robust to changes in the mixed layer depth criterion, though the absolute values of the critical light levels we derive would change.

[12] When compared against chl *a* values, the Argo profiles were further filtered. Profiles in which the mixed layer depth was too sensitive to the choice of criteria used to find it were removed, as in such cases it is not clear what light level the surface phytoplankton are experiencing. Profiles were not used if mixed layer depth changed by  $>20\%$  for  $\Delta\sigma = 0.03 \text{ kg m}^{-3}$  or  $>50\%$  for  $\Delta\sigma = 0.02 \text{ kg m}^{-3}$  relative to

our  $\Delta\sigma = 0.05 \text{ kg m}^{-3}$  criterion. This leaves 46,574 profiles. In all other places in this study, all mixed layer depths are used, so this filtering does not bias other plots.

[13] Satellite ocean color and irradiance data were obtained from <http://oceancolor.gsfc.nasa.gov> (SeaWiFS PAR and chl *a*, version 5.2 (July 2007), and merged SeaWiFS and MODIS chl *a* (MODIS version 1.1, August 2005)). All data are 8 day, 9 km, level 3 mapped images. The merged product from NASA was used for the period 2003–2007, and SeaWiFS chl *a* data were used for 2008. For this work, the increased coverage obtained using two sources was considered to outweigh the issues of differing calibrations between the sources. There are 40,572 profiles that match the above criteria and also have SeaWiFS PAR data, which pass simple quality checks to be within range for a given latitude and date. A total of 21,609 profiles also have colocated chl *a* data. Most profiles without PAR data are during 2008 when there are gaps in the SeaWiFS coverage. Cloud cover and short daylight hours in winter lead to fewer matchups with chl *a* data. Spikes in satellite chl *a* data were filtered by rejecting profiles in which the chl *a* differs by  $>30\%$  from the surrounding 12 pixels, if either the point or surrounding values were in the range  $0.2\text{--}2 \text{ mg m}^{-3}$ . Outside of this range, percentage variability is high, but the data points were considered valid as representing either “low” or “high” chlorophyll. This leaves 21,169 profiles.

[14] Satellite chl *a* data are biased low by approximately a factor of 2 in the Southern Ocean [Korb *et al.*, 2004; Venables *et al.*, 2007]. There is a suggestion that this discrepancy is due to pigments other than chl *a* being included in the in situ measurements [Marrari *et al.*, 2006]. Irrespectively, a correction of  $\text{chl} = -0.08 + 2.07 \cdot \text{chl}$ , as found around Crozet and consistent with South Georgia, is applied in this work as the same in situ measurements were used to find equation (1) below. The chl *a* levels chosen for thresholds are relative to the overall data set, so using a different, or no, calibration would lead to different reference chl *a* values being chosen and no significant change to the light levels found.

[15] There are a number of sources of noise and bias in the data used. PAR is biased high when restricting the profiles to those with chl *a* data, as there needs to be clear sky for the satellite to record a chl *a* value. However, this effect is reduced by use of 8 day satellite periods. The mean PAR is increased by  $1.5 \text{ mol photons m}^{-2} \text{ d}^{-1}$  ( $<4\%$  of mean,  $<20\%$  of standard deviation). When comparing against chl *a*, profiles in which PAR has dropped  $>40\%$  relative to the previous 8 day period are excluded, as these may relate to light levels much lower than those responsible for the phytoplankton response. PAR values from SeaWiFS are those reaching the ocean surface. The transmittance through the surface depends on Sun angle, wind speed, and cloud cover [Campbell and Aarup, 1989] and cannot be accounted for fully, but values have been uniformly reduced by 10% to attempt to account for this issue.

## 3. Southern Ocean Mixed Layer Depths

[16] Mixed layer depths have been calculated from Argo profiles across the entire Southern Ocean. Figure 2 shows the mean mixed layer depth across the Southern Ocean for

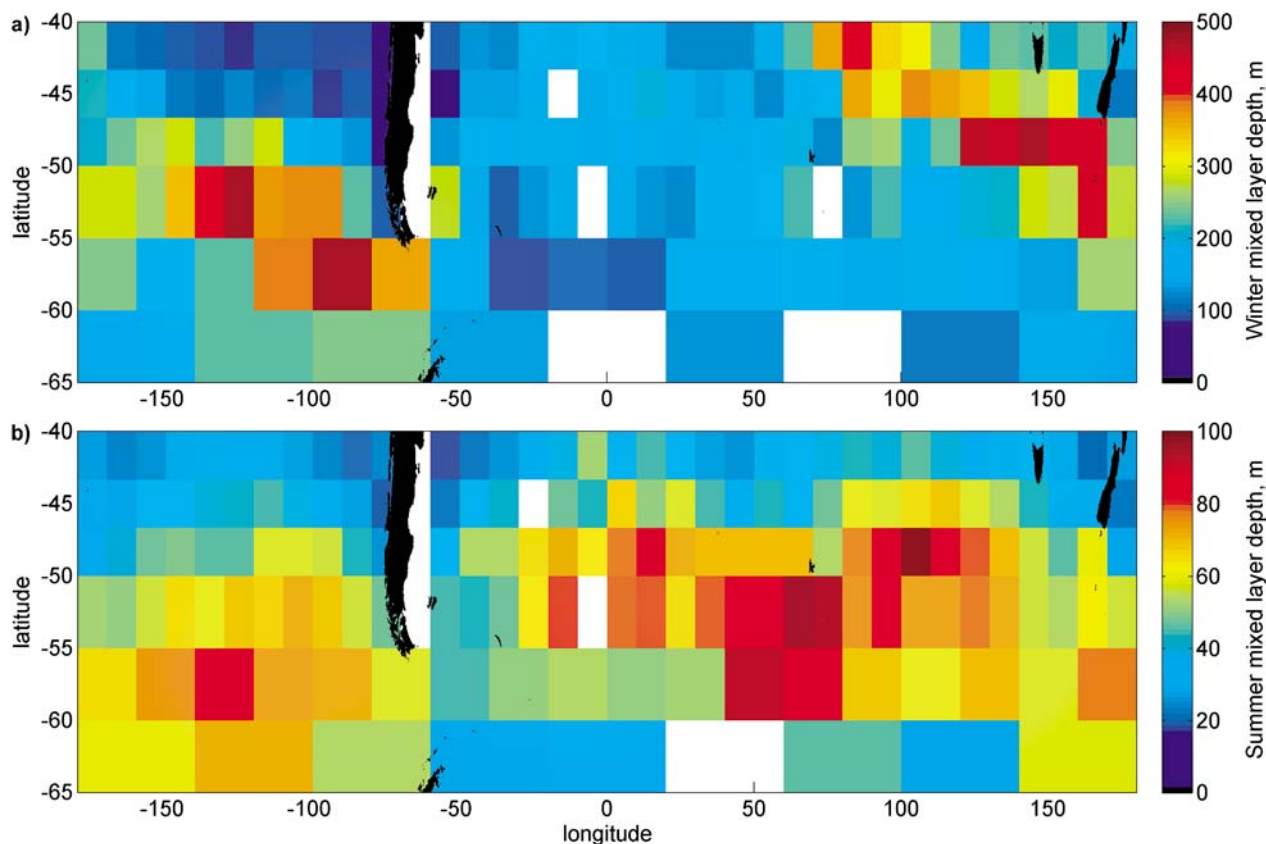


**Figure 2.** Mean mixed layer depths across the Southern Ocean in (a) winter (8 August to 28 September) and (b) summer (1 January to 20 February). Pixels are white if there are too few Argo float profiles, mostly due to depths too shallow for Argo floats ( $<1000$  m).

winter (8 August to 28 September) and summer (1 January to 20 February). The periods were chosen to pick the extreme points of most annual cycles of mixed layer depth. The variability of winter mixed layer depth is striking and has several consequences, potentially most pertinently in the context of Southern Ocean biogeochemistry, those relating to the dilution of iron added at the surface, dilution of phytoplankton standing stocks in autumn, and the mixing back to the surface of carbon exported in the summer.

[17] Summer mixed layer depths are all less than 100 m and show less pronounced variability. Interestingly, summer mixed layers are deepest in areas of low chlorophyll. However, many areas of low summer chlorophyll also have shallow mixed layer depths. In the context of light availability, it should also be noted that the three blooms associated with South Georgia and the Crozet and Kerguelen Islands [Korb *et al.*, 2008; Mongin *et al.*, 2008; Venables *et al.*, 2007] all start well before the summer period represented in Figure 2b, when mixed layers are deeper, e.g., early October when the mixed layer is approximately 90 m for Crozet [Venables *et al.*, 2007].

#### 4. Light Level Sufficient for Naturally Iron-Fertilized Blooms

[18] The naturally iron-fertilized blooms around South Georgia and the Crozet and Kerguelen Islands are high-

nutrient, high-chlorophyll (HNHC) areas that provide an opportunity to study the light requirements of plankton communities in the Southern Ocean, presumably with the effects of iron limitation largely removed. The early development of the Crozet bloom is controlled by the relief of light limitation from an iron-replete area [Planquette *et al.*, 2007; Venables *et al.*, 2007], and the timing of the other blooms [Korb *et al.*, 2004; Mongin *et al.*, 2008] indicates that these are similarly controlled, with blooms starting as light levels increase in spring. Consequently, we assume that these natural blooms were probably close to being light limited at initiation in spring. Note that this situation contrasts markedly with artificial iron releases, where sites were selected so that iron limitation was lifted from an area with high light availability, i.e.,  $\bar{I}_{MLD} \gg I_C$  [Boyd *et al.*, 2007; de Baar *et al.*, 2005].

[19] Using Argo and SeaWiFS data, light requirements for the natural island-associated blooms can be empirically assessed in a number of ways. First, the satellite chl *a* from the time and location of an Argo profile can simply be plotted against the estimated  $\bar{I}_{MLD}$  for the profile. An estimate of  $I_C$  can then be found from the lowest value, which is observed to be associated with significantly enhanced chl *a*. This method has the advantage of a tight match (within 9 km, within 7 days, same year) between the mixed layer depth, PAR, and chl *a*. The method does not, however, capture the light history that allowed the pigment

accumulation. If comparing regions, the described method assumes that light follows a similar seasonal pattern between areas. However, examining the data, this assumption appears valid. Even when using Argo data, there are still relatively few profiles with matching chl *a* data within the HNHC regions, so noise can be introduced through problems with individual data points.

[20] The presence of chlorophyll has a feedback effect on the optical properties of the mixed layer by increasing the attenuation of light and so causing self-shading. The aim of this paper is to use the seasonality of enhanced chlorophyll in the HNHC regions as a source of information on how much light is needed to allow enhanced chlorophyll to develop. The reduction in light availability through self-shading is a consequence of enhanced chlorophyll, not a cause, so it should not be considered in assessing an area's potential for sustaining enhanced standing stocks of phytoplankton. We therefore need to assess the light in a manner that is comparable between high- and low-chlorophyll areas. To do this, we use a constant attenuation, typical of winter or HNLC chlorophyll concentrations of  $0.16 \text{ mg m}^{-3}$ , when comparing high- and low-chlorophyll areas. We refer to the light levels found by this approach as “potential” mixed layer irradiance ( $\bar{I}_{\text{MLD}_p}$ ). However, when examining upper limits to phytoplankton concentrations in the mixed layer due to self-shading, attenuation has to be considered as a function of chlorophyll concentration.

[21] Using  $\bar{I}_{\text{MLD}_p}$  has an added advantage in that it does not require surface chlorophyll data to estimate the attenuation. Consequently, many more profiles with mixed layer depth and surface PAR can be used, including most winter profiles in which chlorophyll data are unavailable. Using a similar argument to that above, a potential critical irradiance ( $I_{\text{C}_p}$ ) can thus be estimated. If  $\bar{I}_{\text{MLD}_p}$  is consistently greater than  $I_{\text{C}_p}$  without an observed net accumulation in chl *a* concentrations, then another factor is most likely limiting increases in the standing stock of chl *a*. Note that we make no a priori assumptions as to what this other factor limiting biomass accumulation may be. High loss rates caused by intense grazing or iron limitation of photosynthesis are just two possibilities. Rather, we make the argument that a given potential light availability was sufficient to allow biomass accumulation to bloom levels in the HNHC areas. Consequently, if the potential light availability is greater than this value elsewhere in the absence of a bloom, then light cannot have been the proximal limiting factor.

[22] An alternative method was described by Siegel *et al.* [2002]. This method, based on classical critical depth theory [Sverdrup, 1953], assumes that  $\bar{I}_{\text{MLD}}$  at the time of the start of the spring increase in chl *a* should provide a good approximation for  $I_{\text{C}}$ . This approach is more in keeping with prior work [Sverdrup, 1953; Siegel *et al.*, 2002] and allows use of all chl *a* data and Argo profiles to look at the progression of light availability with time. However, some of the close spatial and temporal links between the chl *a* and the mixed layer mean light availability are lost. A large spread in  $\bar{I}_{\text{MLD}}$  and chl *a* values is also observed at the initiation of the spring bloom, as the water column restratifies, potentially leading to very rapid reductions in mixed layer depth. The results are therefore sensitive to the statistics and criteria used and any subsampling biases. In theory,  $I_{\text{C}}$  calculated by this method should be similar to the

first method outlined above, in which self-shading effects on attenuation are taken into account. Because of differing strengths and weaknesses, we used both methods and obtained similar results. Moreover, our derived values of  $I_{\text{C}}$  were comparable to published values, further strengthening confidence in our conclusions.

#### 4.1. Mixed Layer Irradiance

[23] Calculations of  $\bar{I}_{\text{MLD}}$  were made using an exponential attenuation of light, integrating the light over the mixed layer depth, and then dividing by the mixed layer depth. This leaves the units as mol photons  $\text{d}^{-1} \text{ m}^{-2}$ , the same as for surface PAR data. The diffuse downwelling attenuation coefficient,  $K_d$ , is assumed to be constant through the mixed layer and is estimated using an empirical relationship found using in situ light profiles and surface chl *a* measurements from the Crozet Natural Iron Bloom and Export Experiment (CROZEX) research cruises D285 and D286 [Moore *et al.*, 2007a] and around South Georgia [Korb *et al.*, 2008]:

$$K_d = 0.05 + 0.057 \text{chl}^{0.58},$$

$$n = 237; r^2 = 0.74; 0.05 < \text{chl } a < 14 \text{ mg m}^{-3}. \quad (1)$$

[24] From this, together with satellite PAR,  $I_{\text{surf}}$ , and mixed layer depth,  $h$ , the mean light availability ( $\bar{I}_{\text{MLD}}$ ) in the mixed layer can be calculated as follows:

$$\bar{I}_{\text{MLD}} = \frac{1}{h} \int_0^h I_{\text{surf}} e^{-K_d z} dz$$

$$\bar{I}_{\text{MLD}} = \frac{I_{\text{surf}}}{K_d h} (1 - e^{-K_d h}). \quad (2)$$

[25] When we have assumed a fixed  $K_d$ , representing a typical winter chl *a* standing stock to allow for direct comparisons of high- and low-chl *a* areas and to include profiles without chl *a* data, we denote the average irradiance estimated from equation (2) as  $\bar{I}_{\text{MLD}_p}$  rather than  $\bar{I}_{\text{MLD}}$ .

#### 4.2. High-Nutrient, High-Chlorophyll Areas

[26] Figure 1 clearly shows that the areas downstream of South Georgia ( $50^\circ\text{S}$ – $58^\circ\text{S}$ ,  $25^\circ\text{W}$ – $45^\circ\text{W}$ ) and the Crozet ( $43^\circ\text{S}$ – $47^\circ\text{S}$ ,  $40^\circ\text{E}$ – $60^\circ\text{E}$ ) and Kerguelen ( $45^\circ\text{S}$ – $55^\circ\text{S}$ ,  $65^\circ\text{E}$ – $85^\circ\text{E}$ ) Islands have exceptionally high chl *a* concentrations relative to the prevailing HNLC conditions in the Southern Ocean. The light availability that triggers and maintains the blooms in the HNHC areas can be used as a guide to assess the potential for light limitation elsewhere in the Southern Ocean. Equally, any explanation of the generally low chl *a* in HNLC regions has to be consistent with these exceptions observed around these island systems.

[27] Figure 3 shows the relationship between the chl *a* standing stock and  $\bar{I}_{\text{MLD}_p}$  around the three HNHC island systems associated with marked blooms. Within these plots, the light attenuation is fixed at a value corresponding to  $0.16 \text{ mg m}^{-3}$  chl *a*, so that the irradiance threshold ( $I_{\text{C}_p}$ ) for bloom initiation above a “background” chlorophyll standing stock can be found. Performing such an analysis allows direct comparison of  $\bar{I}_{\text{MLD}_p}$  in both high- and low-chlorophyll areas. In the context of this analysis, the exact value for the background chlorophyll, and hence attenuation

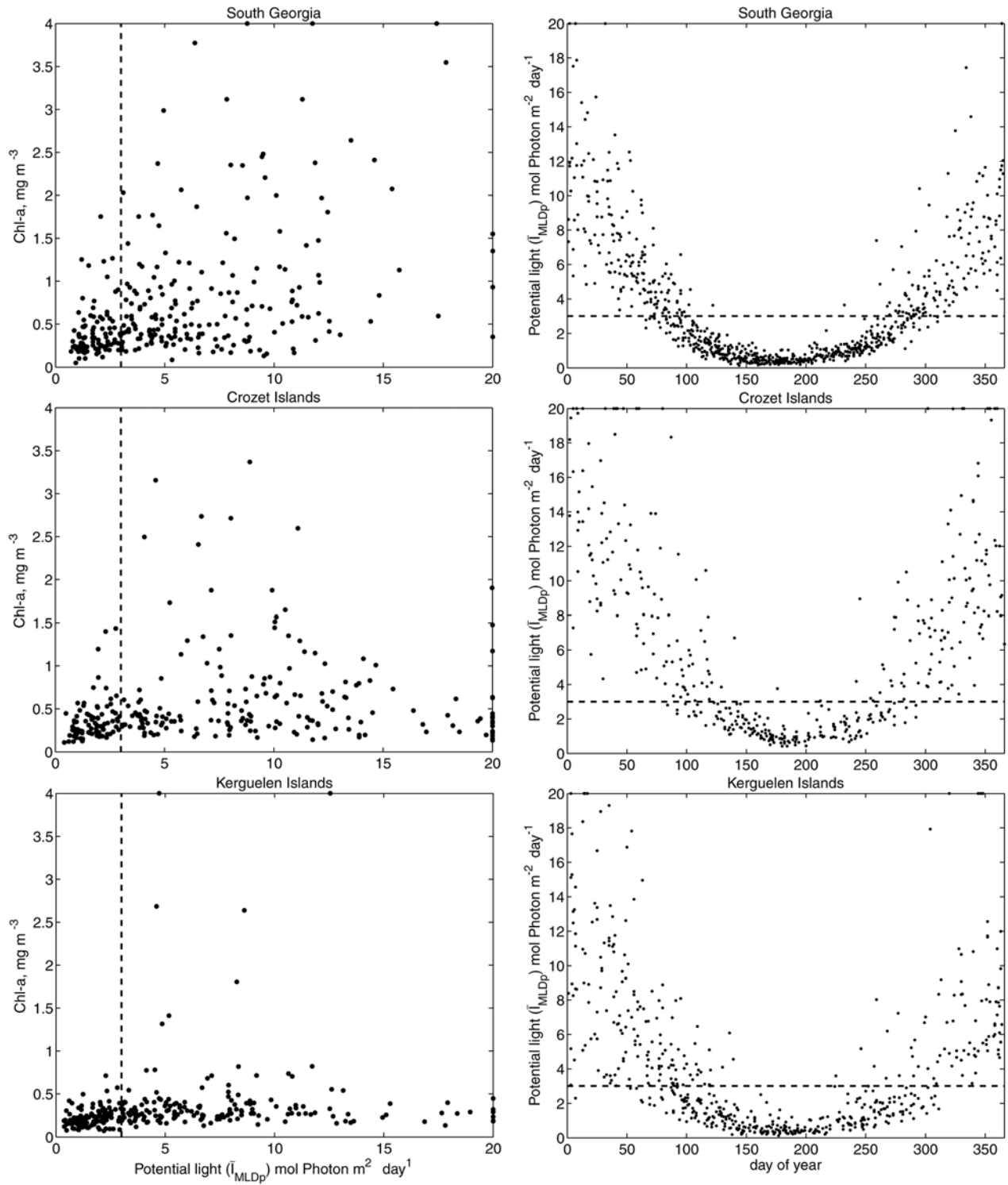


**Figure 3.** The chl *a* versus  $\bar{I}_{MLDP}$  and  $\bar{I}_{MLDP}$  versus time plots for HNHC areas. The line  $\bar{I}_{MLDP} = 3$  mol photons m<sup>-2</sup> d<sup>-1</sup> is added to all plots as a guide.

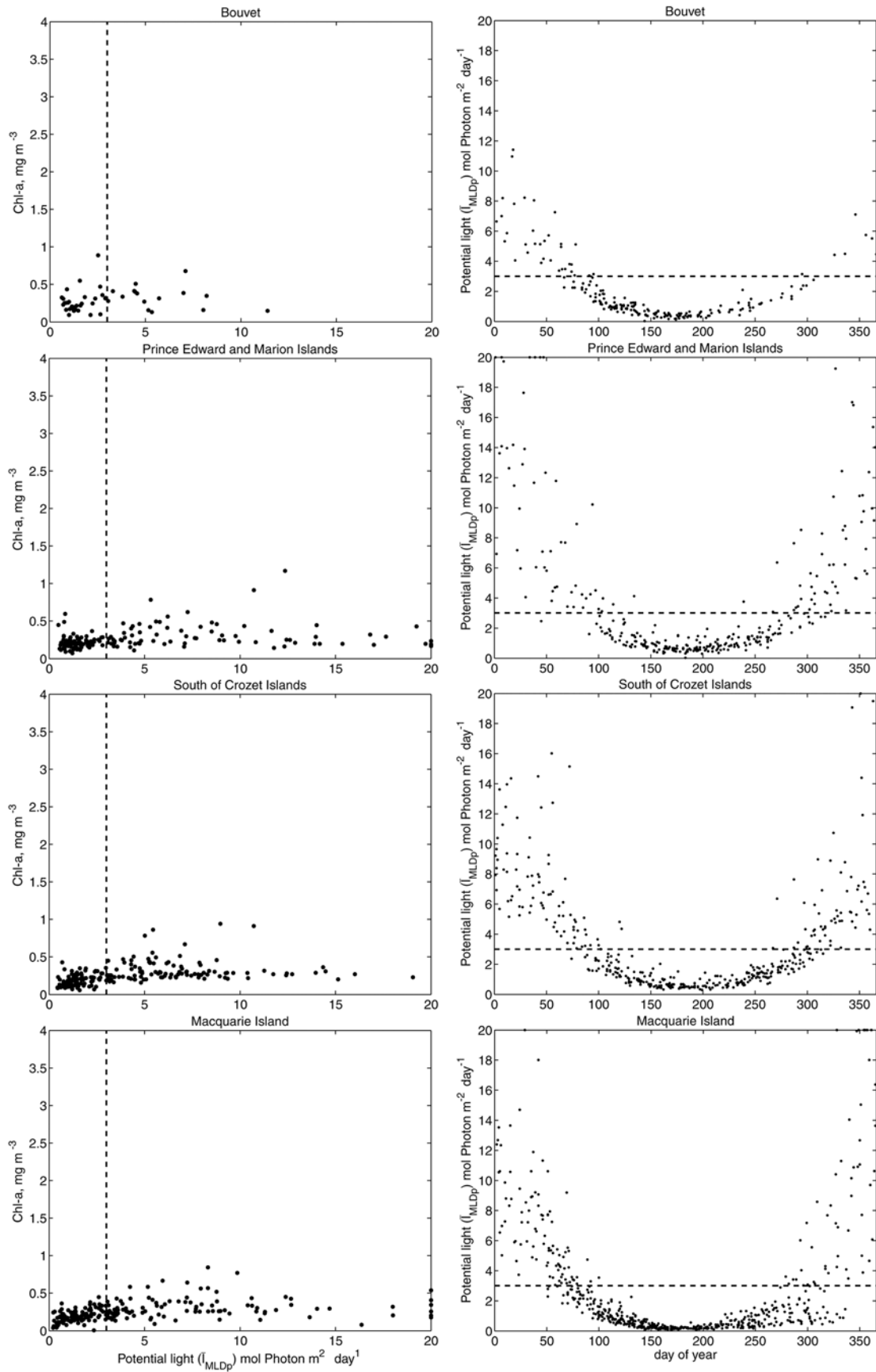


**Figure 4.** The chl *a* versus  $\bar{I}_{MLDP}$  and  $\bar{I}_{MLDP}$  versus time plots for areas close to subantarctic islands where chl *a* is low. The line  $\bar{I}_{MLDP} = 3$  mol photons m<sup>-2</sup> d<sup>-1</sup> is added to all plots as a guide.

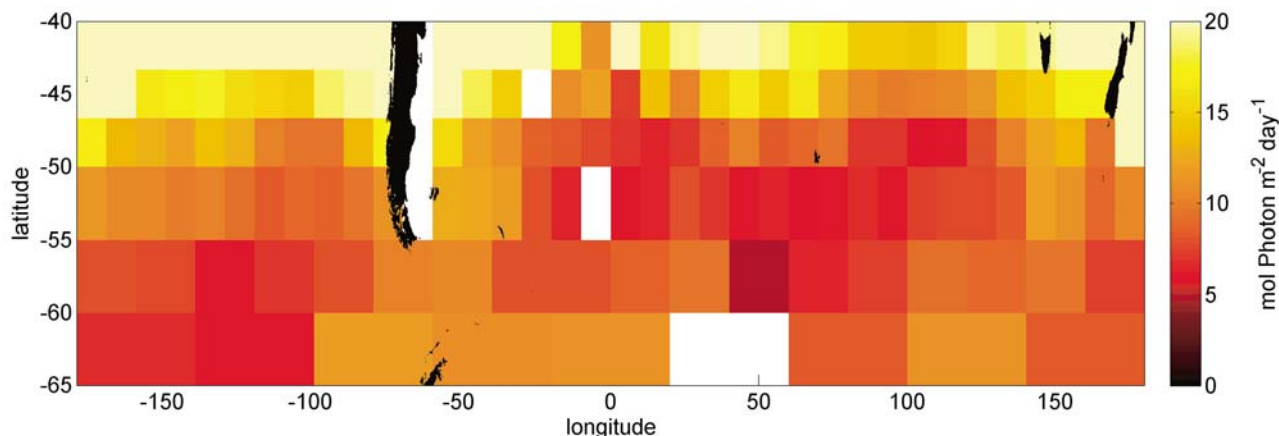


**Figure 5.** Summer (1 January to 20 February)  $\bar{I}_{MLDP}$  across the Southern Ocean. Pixels are white if there are too few Argo float profiles, mostly due to depths too shallow for Argo floats (<1000 m).

coefficient, is not important, so long as the same value is used in both creating and applying the irradiance threshold. In all three island systems, high ( $>2 \text{ mg m}^{-3}$ ) chl *a* concentrations were found when  $\bar{I}_{MLDP} > 3 \text{ mol photons m}^{-2} \text{ d}^{-1}$ . Therefore, by analogy with the HNHC island bloom regions, if chl *a* remains low in other times and regions where the value of  $\bar{I}_{MLDP}$  is consistently  $>3 \text{ mol photons m}^{-2} \text{ d}^{-1}$ , we surmise that a factor other than light availability must be controlling the standing stock.

[28] The annual cycles of potential light availability are also shown in Figure 3. These can be found year-round as the only satellite data used are SeaWiFS PAR, which are available throughout the year and without cloud gaps.

## 5. Light Availability in Low-Chlorophyll Areas

### 5.1. Other Subantarctic Islands

[29] Figure 1 shows the prevailing low-chl *a* conditions in the Southern Ocean. The value for  $I_{Cp}$  ( $3 \text{ mol photons m}^{-2} \text{ d}^{-1}$ ) found above provides a means to assess the contribution of light limitation as the proximal control on chl *a* concentrations in these HNLC areas. We argue that biomass accumulation in these areas is not proximally light limited during any period where the  $\bar{I}_{MLDP} > 3 \text{ mol photons m}^{-2} \text{ d}^{-1}$ , as this light level is sufficient to support enhanced chlorophyll in naturally iron-fertilized blooms.

[30] Figure 4 shows that  $\bar{I}_{MLDP}$  does exceed  $3 \text{ mol photons m}^{-2} \text{ d}^{-1}$  close to the Bouvet ( $51^{\circ}\text{S}$ – $57^{\circ}\text{S}$ ,  $1^{\circ}\text{E}$ – $10^{\circ}\text{E}$ ), Prince Edward ( $44^{\circ}\text{S}$ – $51^{\circ}\text{S}$ ,  $35^{\circ}\text{E}$ – $45^{\circ}\text{E}$ ), and Macquarie ( $52^{\circ}\text{S}$ – $59^{\circ}\text{S}$ ,  $156^{\circ}\text{E}$ – $168^{\circ}\text{E}$ ) islands or south of the Crozet Islands ( $47^{\circ}\text{S}$ – $50^{\circ}\text{S}$ ,  $40^{\circ}\text{E}$ – $60^{\circ}\text{E}$ ) (other islands have too few Argo profiles because of shallow shelves around the islands). Despite this sufficient light level, there is a much lower chl *a* standing stock. The standing stock of chlorophyll in these areas is therefore limited by a factor other than light through the summer. The region south of the Crozet Plateau, which is upstream of land influences [Pollard *et al.*, 2007], was used as the low-iron and hence chl *a* control area for the Crozet Natural Iron Bloom and Export Experiment (CROZEX) project [Venables *et al.*, 2007], and the current approach confirms that biomass accumulation in this region was not restricted by light availability.

[31] From the results of CROZEX [Moore *et al.*, 2007b; Planquette *et al.*, 2007], Kerguelen Ocean and Plateau Compared Study (KEOPS) [Blain *et al.*, 2007], and artificial iron enrichment [de Baar *et al.*, 2005] experiments, the proximal limitation is most likely iron. Although restriction of overall standing stock by intense grazing pressure may remain a possibility for maintaining HNLC conditions, the contrast between bloom and “nonbloom” island systems would require significantly enhanced grazing around those lacking blooms. Moreover, grazing by larger zooplankton, including krill, is actually higher in the bloom region around South Georgia than surrounding areas [Atkinson *et al.*, 2004]. The apparent variation in the iron input or retention in the surface layer around the different islands is presumably linked to differences in geology or hydrology of the islands or associated plateau, the interaction of physical circulation patterns, and topography. Dilution of iron within deep winter mixed layers may also play a role; however, it would be difficult to reconcile this with the summer situation (Figure 1).

### 5.2. Light Availability Across Southern Ocean

[32] Figure 5 shows the distribution of  $\bar{I}_{MLDP}$  in summer (1 January to 20 February) across the Southern Ocean. It can be seen that in all areas the mean exceeds the value for  $I_{Cp}$  estimated above. Consequently, we can conclude that biomass accumulation is not solely limited by light availability during this period for any area of the Southern Ocean.

[33] It is also possible to map the period where  $\bar{I}_{MLDP} > I_{Cp}$  (Figure 6). The spatial resolution varies with the density of Argo profiles to ensure sufficient data through the annual cycle. For each area, the period where  $\bar{I}_{MLDP} > I_{Cp}$  was found by combining data from different years, splitting the year into 10 day intervals (or 20 days where  $<100$  Argo profiles exist in an area), and finding the mean  $\bar{I}_{MLDP}$  across all the profiles in each area and time period. We refer to these values as  $\bar{I}_{MLDP}$ . For some of the 171 areas we used, there are still gaps in the time series of  $\bar{I}_{MLDP}$  where there are no Argo profiles. When gaps were for less than 20 day intervals, we filled them by linearly interpolating from the surrounding data. In 10 areas, there are longer periods wholly within the winter or summer periods ( $\bar{I}_{MLDP} > 3 \text{ mol photons m}^{-2} \text{ d}^{-1}$ ) for that area

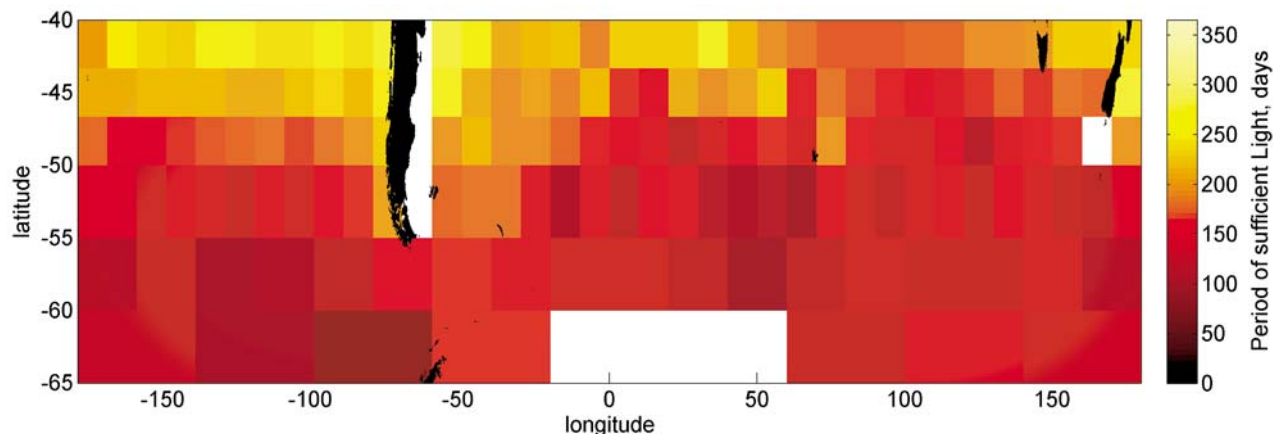


**Figure 6.** Period of sufficient light availability ( $\bar{I}_{MLDP} > I_{Cp}$ ) across the Southern Ocean. Pixels are white if there are too few Argo float profiles.

before and after the period and for areas east and west during the period of missing data. For these areas, the gaps were filled by linear interpolation after manual checking. Seven areas have insufficient profiles because of shelf seas or ice cover and are shown as white pixels in Figures 5 and 6.

[34] The period of sufficient potential light availability was then calculated as the duration of the intervals where  $\bar{I}_{MLDP} > I_{Cp}$ , linearly interpolating between the intervals at each end of the period. The result is shown in Figure 6 and demonstrates a lack of proximal sole light limitation across the entire Southern Ocean. The mean periods for the latitude bands, from the north, are 240, 211, 179, 148, 137, and 135 days for  $I_{Cp} = 3$  mol photons  $m^{-2} d^{-1}$ . The minimum

period of sufficient potential light availability in any area is 97 days. A stricter criterion, of  $I_{Cp} = 5$  mol photons  $m^{-2} d^{-1}$ , reduces these times by approximately 40 days across all latitudes, with a minimum period of 37 days. A weaker criterion, of  $I_{Cp} = 2$  mol photons  $m^{-2} d^{-1}$ , increases the periods by approximately 30 days, with a minimum period of 140 days. The conclusion is therefore robust to the range of possible values that could be selected for  $I_{Cp}$ .

[35] In comparison, the main bloom phase associated with the Crozet Islands collapses within 120 days of initiation [Venables *et al.*, 2007]. The Crozet bloom was responsible for the removal of approximately  $0.6$  mol  $NO_3^- m^{-2}$  and enhanced carbon export at 200 m by  $0.34$  mol  $m^{-2}$  [Pollard

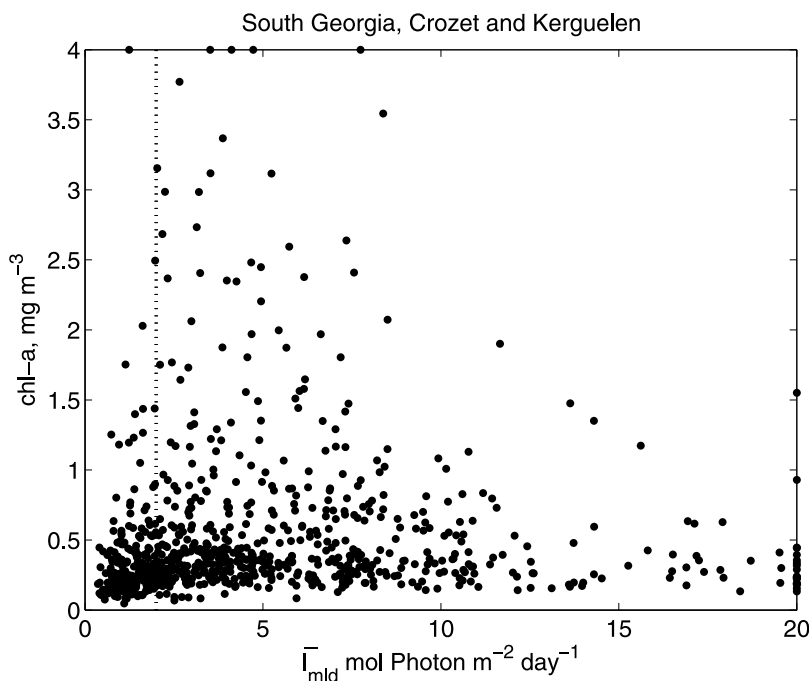


**Figure 7.** The chl *a* against  $\bar{I}_{MLD}$  for the three HNHC areas, accounting for attenuation caused by chlorophyll and satellite calibration (chl *a* values are doubled). Note that for plotting reasons, chl *a* values  $>4$   $mg m^{-3}$  are plotted at  $4$   $mg m^{-3}$  and irradiance is similarly constrained to  $20$  mol photons  $m^{-2} d^{-1}$ .

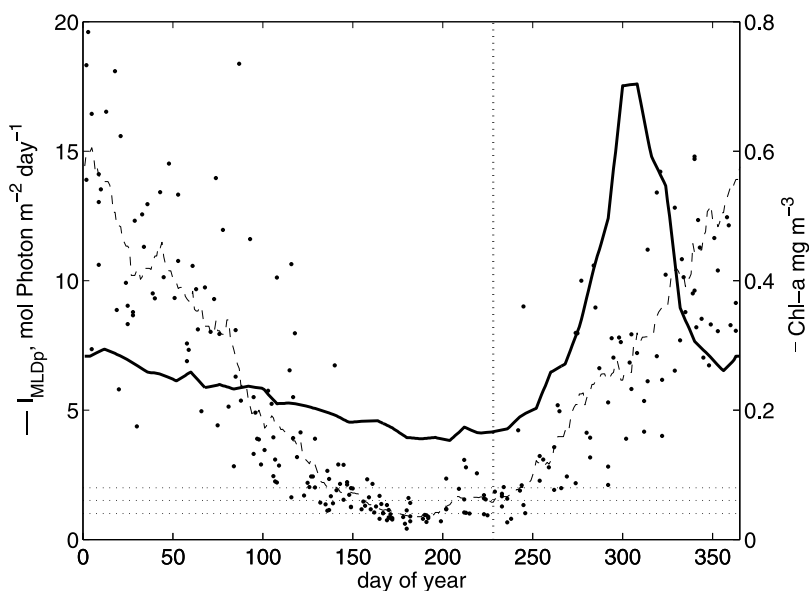


**Figure 8.** Example area showing the process of finding the mixed layer-averaged light ( $\bar{I}_{MLD}$ ) (28 day running average (dashed line) of the individual Argo profiles (dots)) associated with the start of the spring increase in chl *a* (solid line, plotted against midpoints of 8 day periods). The vertical dotted line shows the date found for the start of the increase. The horizontal lines are at 1, 1.5, and 2 mol photons  $m^{-2} d^{-1}$  as a guide.

*et al.*, 2009]. Consequently, we conclude that there is likely sufficient light to support a similar bloom almost anywhere in the Southern Ocean and all areas could support enhanced phytoplankton biomass for at least 3 months. The integrated standing stock in the Crozet bloom, which itself ends before light is limiting [Venables *et al.*, 2007], is two-and-a-half times greater than in the low-chlorophyll area to the south, which is typical of HNLC conditions (Figure 1). Winter light limitation in this area is less than 6 months, so even if light was nonlimiting south of Crozet throughout winter, the integrated standing stock would still be lower than in the bloom area. Therefore, we conclude that light does not limit annually integrated standing stocks of chlorophyll, though winter limitation produces some downward influence.

### 5.3. Compensation Irradiance

[36] Section 4 finds a sufficient condition for light availability. The value of 3 mol photons  $m^{-2} d^{-1}$  for  $I_{Cp}$  is not, however, an accurate measure of the minimum light level required for net growth at bloom initiation, as self-shading was not considered and, as described above, the threshold for defining enhanced chl *a* is significantly greater than winter values. The analysis based on  $I_{Cp}$  thus provides an unambiguous measure to test for light limiting the development of large blooms in low-chl *a* areas but is not appropriate for assessing the timing of bloom onset or effects of self-shading at high-chl *a* concentrations [de Baar *et al.*, 2005; Huismann, 1999]. Equally, light levels exceeding a critical threshold is a necessary, but not sufficient, condition for a bloom. The net growth may be very slow and soon stopped by self-shading effects reducing light levels back to the critical level, hence the use of the above method for assessing the potential for bloom formation.

[37] As described in section 4, there are two possible approaches for empirically estimating the actual community compensation irradiance,  $I_C$ . The first method involves repeating the analysis performed in section 4.2 for  $I_{Cp}$  in high-chl *a* areas with an attenuation coefficient that is a function of chl *a* concentration (equation (1)). Figure 7 shows the result of plotting  $\bar{I}_{MLD}$  against chl *a*, for South Georgia, Crozet, and Kerguelen combined. This analysis suggests an estimate of 2 mol photons  $m^{-2} d^{-1}$  for  $I_C$ .

[38] The second method of finding  $I_C$  detailed in section 4 is comparable to this result: to first order the irradiance level at which net growth starts because of increasing mean light levels within a mixed layer should be the same as that at which net growth stops because of self-shading development within a bloom. However, the self-shading limit during bloom development will be approached asymptotically with light limitation gradually increasing, if surface irradiance and mixed layer conditions were constant, and so estimates from observations are likely to be higher than the limiting irradiance for bloom initiation. Changes in loss terms through the season could also influence the comparison. Absolute grazing pressure most likely increases through the season as zooplankton grow and reproduce, but as phytoplankton biomass increases as well, it is not clear without close study whether the grazing rate per unit of phytoplankton biomass increases or decreases, leading to higher or lower critical light levels, respectively.

[39] We used a similar method to that of Siegel *et al.* [2002] to find the compensation irradiance at bloom initiation. Using the data described above and the same areas as Figure 6 (but restricted to south of 43°S), an estimate of 1.4 mol photons  $m^{-2} d^{-1}$  (SD = 0.6, 21 areas used) is found. This is lower than the self-shading limit found above, as would be expected. Figure 8 shows an example

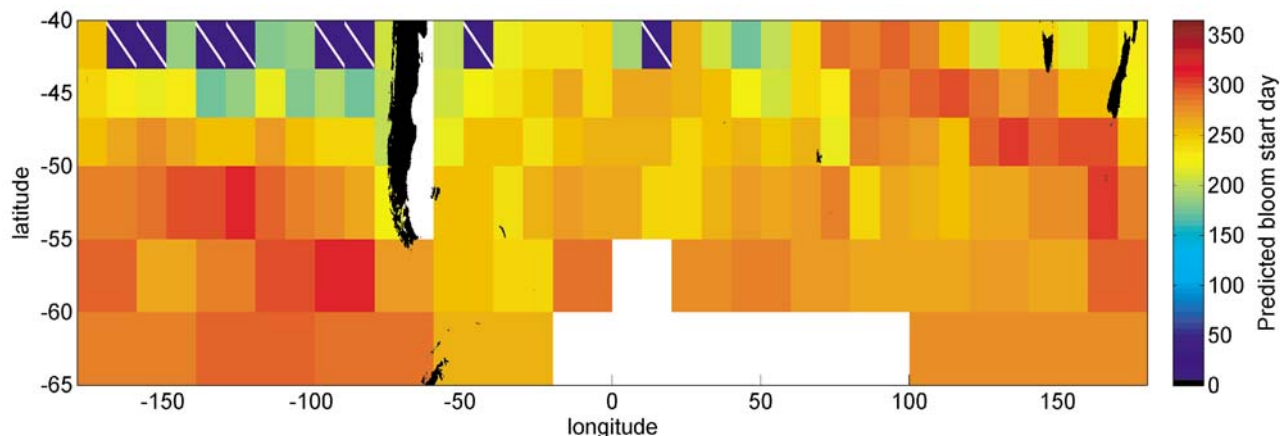


**Figure 9.** Day of year for light reaching  $1.4 \text{ mol photons m}^{-2} \text{ d}^{-1}$  across the Southern Ocean. Pixels that are blue with a white stripe show areas where light does not drop below the critical level found. There are no data for white pixels.

of the process of finding the light availability at the time of the beginning of the spring increase in chl *a*. The time of bloom initiation was selected as the start of at least three 8 day periods of consistent chl *a* increase (SeaWiFS chl *a* data averaged over 2003–2007 to match the Argo period and avoid the data outages of 2008). Winter chl *a* values are absent south of  $47^{\circ}\text{S}$ , so it is not possible to use an identical method to Siegel *et al.* [2002] for finding the time of bloom initiation. This method also picks the start of the increase rather than when the increase passes a threshold. Calculations were performed for regions where there was a period of sustained chl *a* increase and the peak averaged chl *a* exceeded  $0.45 \text{ mg m}^{-3}$  within the annual cycle. The light at this time was found after applying a 14 day running mean to the Argo/SeaWiFS-derived  $\bar{I}_{\text{MLDp}}$ . Since this was calculated using an attenuation coefficient corresponding to  $0.16 \text{ mg m}^{-3}$  of chl *a*, this value will give a good approximation of  $\bar{I}_{\text{MLD}}$  at bloom initiation, when chl *a* is  $0.16 \text{ mg m}^{-3}$ , on average. Consequently, the value of  $\bar{I}_{\text{MLD}}$  at bloom initiation is taken as  $I_C$ .

[40] Siegel *et al.* [2002] in the North Atlantic, using climatological mixed layer depths, found a similar result of  $1.3 \text{ mol photons m}^{-2} \text{ d}^{-1}$  (SD =  $0.3 \text{ mol photons m}^{-2} \text{ d}^{-1}$ ) for  $I_C$ . In addition, these values are supported by results from incubation experiments during Southern Ocean Iron Enrichment Experiment (SOIREE) [Boyd *et al.*, 2000]. Phytoplankton at a light level equivalent to 65 m ( $\bar{I}_{\text{MLD}} = 3 \text{ mol photons m}^{-2} \text{ d}^{-1}$ ) grew strongly, whereas the bottle at the equivalent light of a 100 m mixed layer depth ( $\bar{I}_{\text{MLD}} = 2 \text{ mol photons m}^{-2} \text{ d}^{-1}$ ) showed only a small increase in chl *a*.

[41] The value for  $I_C$  derived from the second approach provides a method to estimate when a bloom would start, in the absence of other (iron) limitation. This is shown in Figure 9, although it is not necessarily a valid method for the most northerly band,  $40^{\circ}\text{S}$ – $43^{\circ}\text{S}$ , because this area was excluded from finding  $I_C$ , hence the mean value for this latitude band is presented in parentheses. The mean days of year for each latitude band, from the north, are (230), 239, 259, 270, 276, and 279. Varying  $I_C$  by  $\pm 1$  SD delays these start dates by approximately 15 days for  $I_C = 2 \text{ mol photons m}^{-2} \text{ d}^{-1}$  or brings them forward by about 20 days

for  $I_C = 0.8 \text{ mol photons m}^{-2} \text{ d}^{-1}$ . A correlation can be seen with the deep winter mixed layer depths in Figure 2a.

## 6. Conclusions

[42] This study demonstrates that for a significant period of the year, at least 3 months, the HNLC Southern Ocean is not proximately light limited. Consequently, the relief of likely widespread iron limitation could lead to significant increases in chlorophyll, similar to that seen around South Georgia and the Crozet and Kerguelen Islands. The prolonged periods where the lowest recorded light level is greater than our estimated value for  $I_C$  further suggest that variations in the mixed layer may not be sufficient to maintain the low chlorophyll in the HNLC regions [Platt *et al.*, 2003]. Indeed, the accumulation of chl *a* does not appear to be restricted by such a process in the HNLC regions downstream from the island systems associated with large blooms, which are subject to similar wind stress as the rest of the Southern Ocean [Risien and Chelton, 2008] and which show a similar annual cycle in light availability.

[43] The lack of proximal light limitation suggests that widespread, seasonally sustained iron addition to the HNLC areas, through climatic changes, volcanism, or geoengineering, would lead to levels of biological production similar to those observed in the naturally iron fertilized blooms. Further study of these blooms is therefore valuable in assessing the potential impacts of this increased biological production on the carbon cycle, higher trophic levels, and nutrient utilization.

[44] **Acknowledgments.** Argo data were collected and made freely available by the International Argo Project and the national programs that contribute to it (<http://www.argo.ucsd.edu>, <http://argo.jcommops.org>). Argo is a pilot program of the Global Ocean Observing System. SeaWiFS and MODIS-aqua data were provided by the SeaWiFS Project, NASA Goddard Space Flight Center, and ORBIMAGE. This paper is a contribution to the BAS Discovery 2010 program.

## References

Atkinson, A., V. Siegel, E. Pakhomov, and P. Rothery (2004), Long-term decline in krill stock and increase in salps within the Southern Ocean, *Nature*, 432, 100–103, doi:10.1038/nature02996.

- Aumont, O., and L. Bopp (2006), Globalizing from ocean in situ iron fertilization studies, *Global Biogeochem. Cycles*, 20, GB2017, doi:10.1029/2005GB002591.
- Blain, S., et al. (2007), Effects of natural iron fertilization on carbon sequestration in the Southern Ocean, *Nature*, 446, 1070–1074, doi:10.1038/nature05700.
- Boyd, P. W., et al. (2000), A mesoscale phytoplankton bloom in the polar Southern Ocean stimulated by iron fertilization, *Nature*, 407, 695–702, doi:10.1038/35037500.
- Boyd, P. W., et al. (2004), The decline and fate of an iron-induced subarctic phytoplankton bloom, *Nature*, 428, 549–553, doi:10.1038/nature02437.
- Boyd, P. W., et al. (2007), Mesoscale iron enrichment experiments 1993–2005: Synthesis and future directions, *Science*, 315, 612–617, doi:10.1126/science.1131669.
- Brainerd, K. E., and M. C. Gregg (1995), Surface mixed and mixing layer depths, *Deep Sea Res., Part I*, 42, 1521–1543, doi:10.1016/0967-0637(95)00068-H.
- Campbell, J. W., and T. Aarup (1989), Photosynthetically available radiation at high latitudes, *Limnol. Oceanogr.*, 34, 1490–1499.
- Coale, K. H., et al. (1996), A massive phytoplankton bloom induced by an ecosystem-scale iron fertilisation experiment in the equatorial Pacific Ocean, *Nature*, 383, 495–501, doi:10.1038/383495a0.
- Coale, K. H., et al. (2004), Southern Ocean iron enrichment experiment: Carbon cycling in high and low-Si waters, *Science*, 304, 408–414, doi:10.1126/science.1089778.
- de Baar, H. J. W., et al. (2005), Synthesis of iron fertilization experiments: From the Iron Age in the Age of Enlightenment, *J. Geophys. Res.*, 110, C09S16, doi:10.1029/2004JC002601.
- Duce, R. A., and N. W. Tindale (1991), Atmospheric transport of iron and its deposition in the Ocean, *Limnol. Oceanogr.*, 36, 1715–1726.
- Fennel, K., M. R. Abbott, Y. H. Spitz, J. G. Richman, and D. M. Nelson (2003), Modeling controls of phytoplankton production in the southwest Pacific sector of the Southern Ocean, *Deep Sea Res., Part II*, 50, 769–798, doi:10.1016/S0967-0645(02)00594-5.
- Gervais, F., and U. Riebesell (2002), Changes in primary productivity and chlorophyll-a in response to iron fertilization in the Southern Polar Frontal Zone, *Limnol. Oceanogr.*, 47, 1324–1335.
- Holeton, C. L., F. Nédélec, R. Sanders, L. Brown, C. M. Moore, D. P. Stevens, K. J. Heywood, P. J. Statham, and C. H. Lucas (2005), Physiological state of phytoplankton communities in the southwest Atlantic sector of the Southern Ocean, as measured by fast repetition rate fluorometry, *Polar Biol.*, 29, 44–52, doi:10.1007/s00300-005-0028-y.
- Huisman, J. (1999), Population dynamics of light-limited phytoplankton: Microcosm experiments, *Ecology*, 80, 202–210.
- Huisman, J., P. van Oostven, and F. J. Weissing (1999), Critical depth and critical turbulence: Two different mechanisms for the development of phytoplankton blooms, *Limnol. Oceanogr.*, 44, 1781–1787.
- Jickells, T. D., et al. (2005), Global iron connections between desert dust, ocean biogeochemistry, and climate, *Science*, 308, 67–71, doi:10.1126/science.1105959.
- Kara, A. B., P. A. Rochford, and H. E. Hurlburt (2000), An optimal definition for ocean mixed layer depth, *J. Geophys. Res.*, 105, 16,803–16,821, doi:10.1029/2000JC900072.
- Kara, A. B., P. A. Rochford, and H. E. Hurlburt (2003), Mixed layer depth variability over the global ocean, *J. Geophys. Res.*, 108(C3), 3079, doi:10.1029/2000JC000736.
- Korb, R. E., and M. J. Whitehouse (2004), Contrasting primary production regimes around South Georgia, Southern Ocean: Large blooms versus high nutrient low chlorophyll waters, *Deep Sea Res., Part I*, 51, 721–738, doi:10.1016/j.dsr.2004.02.006.
- Korb, R. E., M. J. Whitehouse, and P. Ward (2004), SeaWiFS in the Southern Ocean: Spatial and temporal variability in phytoplankton biomass around South Georgia, *Deep Sea Res., Part II*, 51, 99–116, doi:10.1016/j.dsr.2003.04.002.
- Korb, R. E., M. J. Whitehouse, A. Atkinson, and S. E. Thorpe (2008), Magnitude and maintenance of the phytoplankton bloom at South Georgia: A naturally iron-replete environment, *Mar. Ecol. Prog. Ser.*, 368, 75–91, doi:10.3354/meps07525.
- Lalli, C. M., and T. R. Parsons (1997), *Biological Oceanography: An Introduction*, 2nd ed., 314 pp., Butterworth Heinemann, Oxford, U. K.
- Maldonado, M. T., P. W. Boyd, P. J. Harrison, and N. M. Price (1999), Co-limitation of phytoplankton growth by light and Fe during winter in the NE subarctic Pacific Ocean, *Deep Sea Res., Part II*, 46, 2475–2485, doi:10.1016/S0967-0645(99)00072-7.
- Marrari, M., C. Hu, and K. Daly (2006), Validation of SeaWiFS chlorophyll a concentrations in the Southern Ocean: A revisit, *Remote Sens. Environ.*, 105, 367–375, doi:10.1016/j.rse.2006.07.008.
- Martin, J. H. (1990), Glacial-interglacial CO<sub>2</sub> change: The iron hypothesis, *Paleoceanography*, 5, 1–13, doi:10.1029/PA005i001p00001.
- Martin, J. H., R. M. Gordon, and S. E. Fitzwater (1990), Iron in Antarctic waters, *Nature*, 345, 156–158, doi:10.1038/345156a0.
- Mitchell, B. G., E. A. Brody, O. Holm-Hansen, C. McClain, and J. Bishop (1991), Light limitation of phytoplankton biomass and macronutrient utilization in the Southern Ocean, *Limnol. Oceanogr.*, 36, 1662–1677.
- Mongin, M., E. Molina, and T. W. Trull (2008), Seasonality and scale of the Kerguelen plateau phytoplankton bloom: A remote sensing and modeling analysis of the influence of natural iron fertilization in the Southern Ocean, *Deep Sea Res., Part II*, 55, 880–892, doi:10.1016/j.dsr.2.2007.12.039.
- Moore, C. M., A. E. Hickman, A. J. Poulton, S. Seeyave, and M. Lucas (2007a), Iron-light interactions during the Crozet Natural Iron Bloom and Export Experiment (CROZEX) II: Taxonomic responses and elemental stoichiometry, *Deep Sea Res., Part II*, 54, 2066–2084, doi:10.1016/j.dsr.2.2007.06.015.
- Moore, C. M., S. Seeyave, A. E. Hickman, J. T. Allen, M. Lucas, H. Planquette, R. T. Pollard, and A. J. Poulton (2007b), Iron-light interactions during the Crozet Natural Iron Bloom and Export Experiment (CROZEX) I: Phytoplankton growth and photophysiology, *Deep Sea Res., Part II*, 54, 2045–2065, doi:10.1016/j.dsr.2.2007.06.011.
- Moore, J. K., M. R. Abbott, J. G. Richman, W. O. Smith, T. J. Cowles, K. H. Coale, W. D. Gardner, and R. T. Barber (1999), SeaWiFS satellite ocean color data from the Southern Ocean, *Geophys. Res. Lett.*, 26, 1465–1468, doi:10.1029/1999GL900242.
- Morel, F. M. M., J. G. Rueter, and N. M. Price (1991), Iron nutrition of phytoplankton and its possible importance in the ecology of ocean regions with high nutrient and low biomass, *Oceanography*, 4, 56–61.
- Planquette, H., et al. (2007), Dissolved iron in the vicinity of the Crozet Islands, Southern Ocean, *Deep Sea Res., Part II*, 54, 1999–2019, doi:10.1016/j.dsr.2.2007.06.019.
- Platt, T., S. Sathyendranath, A. M. Edwards, D. S. Broomhead, and O. Ulloa (2003), Nitrate supply and demand in the mixed layer of the ocean, *Mar. Ecol. Prog. Ser.*, 254, 3–9, doi:10.3354/meps254003.
- Pollard, R. T., P. Treguer, and J. Read (2006), Quantifying nutrient supply to the Southern Ocean, *J. Geophys. Res.*, 111, C05011, doi:10.1029/2005JC003076.
- Pollard, R. T., H. J. Venables, J. F. Read, and J. T. Allen (2007), Large scale circulation around the Crozet Plateau controls an annual phytoplankton bloom in the Crozet Basin, *Deep Sea Res., Part II*, 54, 1915–1929, doi:10.1016/j.dsr.2.2007.06.012.
- Pollard, R. T., et al. (2009), Southern Ocean deep-water carbon export enhanced by natural iron fertilization, *Nature*, 457, 577–581, doi:10.1038/nature07716.
- Raven, J. A. (1990), Predictions of MN and Fe use efficiencies of phototrophic growth as a function of light availability for growth and of C assimilation pathway, *New Phytol.*, 116, 1–18, doi:10.1111/j.1469-8137.1990.tb00505.x.
- Risien, C. M., and D. B. Chelton (2008), A global climatology of surface wind and wind stress fields from eight years of QuikSCAT Scatterometer data, *J. Phys. Oceanogr.*, 38, 2379–2413, doi:10.1175/2008JPO3881.1.
- Siegel, D. A., S. C. Doney, and J. A. Yoder (2002), The North Atlantic spring phytoplankton bloom and Sverdrup's critical depth hypothesis, *Science*, 296, 730–733.
- Smetacek, V., and U. Passow (1990), Spring bloom initiation and Sverdrup's critical-depth model, *Limnol. Oceanogr.*, 35, 228–234.
- Strzepek, R. F., and P. J. Harrison (2004), Photosynthetic architecture differs in coastal and oceanic diatoms, *Nature*, 431, 689–692, doi:10.1038/nature02954.
- Sunda, W. G., and S. A. Huntsman (1997), Interrelated influence of iron, light and cell size on marine phytoplankton growth, *Nature*, 390, 389–392, doi:10.1038/37093.
- Sverdrup, H. U. (1953), On conditions for the vernal blooming of phytoplankton, *J. Cons. Cons. Int. Explor. Mer.*, 18, 287–295.
- Tsuda, A., et al. (2003), A mesoscale iron enrichment in the western subarctic Pacific induces a large centric diatom bloom, *Science*, 300, 958–961, doi:10.1126/science.1082000.
- Venables, H. J., R. T. Pollard, and E. E. Popova (2007), Physical conditions controlling the early development of a regular phytoplankton bloom north of the Crozet Plateau, Southern Ocean, *Deep Sea Res., Part II*, 54, 1949–1965, doi:10.1016/j.dsr.2.2007.06.014.

C. M. Moore, National Oceanography Centre, University of Southampton, European Way, Southampton SO14 3ZH, UK.

H. Venables, British Antarctic Survey, High Cross, Madingley Road, Cambridge CB3 0ET, UK. (hvj@bas.ac.uk)